CHEMISTRY OF MATERIALS

ARTICLE

pubs.acs.org/cm

Synthesis and Energy Release of Nitrobenzene-Functionalized Single-Walled Carbon Nanotubes

Joel T. Abrahamson,[†,⊥] Changsik Song,[†,§,⊥] Jenny H. Hu,[†] Jared M. Forman,[†,‡] Sayalee G. Mahajan,[†] Nitish Nair,[†] Wonjoon Choi,[†,∥] Eun-Ji Lee,[§] and Michael S. Strano*[,†]

[†]Department of Chemical Engineering, [‡]Department of Chemistry, and [∥]Department of Mechanical Engineering, Massachusetts Institute of Technology, Cambridge, Massachusetts 02139, United States

[§]Department of Chemistry, Sungkyunkwan University, Suwon 440-746, South Korea

Supporting Information

ABSTRACT: Nanomaterials offer advantages as new fuels and energetic materials because of increased surface areas, enhancement of chemical reactivity that often accompanies a reduction in particle size, and the ability to form composites. Applications include new energy storage devices and power sources. In this work, we report the synthesis of single-walled carbon nanotubes decorated with mono-, di-, and trinitrobenzenes via diazonium chemistry as a means of increasing their energy density. Differential scanning calorimetry confirms thermally initiated energy release from such systems, with no release from control materials. Analysis of calorimetric data shows a statistically lower value of activation energy at low conversion, providing evidence for nanotube-guided chain reactions. Although covalent functionalization introduces defects that tend to scatter electrons and phonons, reducing electrical and thermal conductivity, we show that thermopower waves are still able to rapidly propagate along such decorated nanotubes and produce electrical power. The results offer new ways of storing chemical energy within carbon nanotubes and new conduits for thermopower wave generators.

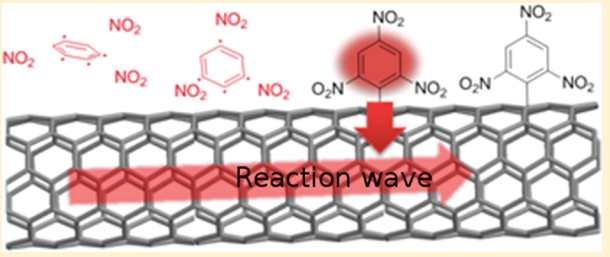

KEYWORDS: carbon nanotubes, nanoenergetic materials, reaction propagation, power source, thermopower waves, energy storage

INTRODUCTION

Engineering materials at the nanometer scale has enabled new technologies, particularly in the area of energy storage and release.[1−4] Nanostructured fuels benefit from increased surface areas, enhancement of chemical reactivity and transport properties, and the ability to form nanocomposites.[5,6] Nanoenergetic materials[7] appear to overcome many limitations of conventional energetic materials, for example, incomplete combustion when diffusive mass transport limits reaction.[8] By applying molecular-scale design principles, the energy density of engineered nanoenergetic materials can be increased compared to conventional materials.[7] A particularly interesting case is an exothermic chemical reaction coupled to a highly thermally conductive nanoconduit. For instance, our group recently demonstrated through modeling, as a proof-of-concept, that reaction rates are accelerated anisotropically when a single-walled carbon nanotube (SWNT) is thermally coupled to a metal oxidation reaction in an annulus of fuel surrounding it.[9] In case of Zr metal, reaction velocity increased from 530 to 5100 mm/s in the direction of the nanotube's length. One-dimensional (1-D) nanoenergetic materials such as these may find new interesting applications such as novel propellants and high-energy materials synthesis by focusing energy at the nanoscale.

Experimental endeavors in our group have resulted in the discovery of a new concept for the conversion of chemical energy to electricity: thermopower waves.[10−12] Using 7-nm shells of energetic material around carbon nanotubes, which have very high axial thermal conductivity, a reaction wave can self-propagate along the length, at a rate amplified by more than 10^4 times the bulk value. Most importantly, this reaction wave produces a concomitant thermopower wave of high power density (>7 kW/kg), resulting in an electrical current along the same direction. The thermopower wave is generated via entrainment of charge carriers by self-sustaining reaction waves in a system where an exothermic fuel is thermally coupled to an anisotropic heat conductor. This emerging concept is expected to overcome the limitations of traditional thermoelectricity and may find use in many unique nanoscale energy sources. Nor is the phenomenon limited to carbon nanotubes; Walia et al. recently demonstrated thermopower waves using nitrocellulose as the fuel and a thin film of Bi_2Te_3 sputtered on alumina as the electrical and heat conductors, respectively.[13] Thus, thermopower waves can be realized in layered geometries as well.

Received: July 8, 2011
Revised: September 7, 2011
Published: September 27, 2011

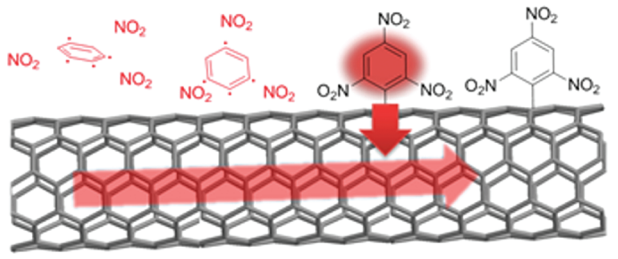

Figure 1. Schematic representation of reaction propagation on a single-walled carbon nanotube decorated with energetic molecules (trinitrobenzenes).

Scheme 1. Synthesis of Nitrophenyl-SWNTs via Diazonium Reactions[a]

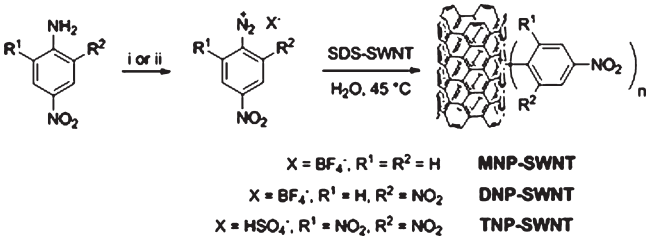

[a] (i) $NOBF_4$, acetonitrile, 0 °C, 4 h (for MNP- and DNP-SWNT). (ii) $NOHSO_4$ ($NaNO_2$ + H_2SO_4), H_2O, room temperature, 3 h (for TNP-SWNT).

Creating new classes of nanoenergetic materials with low dimensionality also stirs interest in the field. One approach is covalently attaching energetic molecules to a nanotube or nanowire, which can serve as a 1-D heat conductor (Figure 1). Energy from a chemical reaction at the one end may propagate through the 1-D conductor, initiating reactions in the attached molecules at the propagating wavefront. Several questions define the performance and function of such systems: (1) how much energy can be stored and released, and how fast can it occur? (2) are tunable 1-D nanoenergetic materials possible (for example, SWNTs decorated with mono-, di-, or trinitroaromatics)? (3) after initiation of a reaction in the system, can the reaction wave self-propagate? (4) can the system support thermopower waves? If so, what are the effects of covalent functionalization of the thermal/electrical conduit? The answers to the above questions will further the understanding of thermopower waves.

This study describes the synthesis of a series of nitrophenyl-decorated SWNTs using diazonium functionalization chemistry. These energetically decorated SWNTs are explored as a nanoscale energy source. Self-propagating reaction waves were launched on the covalently decorated nanoenergetic SWNTs to test thermopower wave generation.

RESULTS AND DISCUSSION

Synthesis of Nitrophenyl-functionalized SWNTs via Diazonium Chemistry. Energetically decorated SWNTs were successfully synthesized utilizing diazonium chemistry.[14−17] As described in Scheme 1, mono-, di-, and trinitrobenzenediazonium salts were first prepared from corresponding anilines. Diazotization of 4-nitroaniline and 2,4-dinitroaniline went smoothly with nitrosonium tetrafluoroborate ($NOBF_4$) in CH_3CN, furnishing mono- and dinitrobenzenediazonium salts, respectively, as a pure, isolable solid.[16] However, the same method did not work for 2,4,6-trinitroaniline, presumably because of significantly weak basicity of the aniline.[18] Strong acidic media seem to be necessary to diazotize such a weak amine, and indeed diazotization of 2,4,6-trinitroaniline was possible with in situ-generated nitrosylsulfuric acid following a method by Matsui and co-workers after a slight modification.[19] However, all attempts to isolate the corresponding diazonium salt proved unsuccessful; thus the diazonium salt solution was utilized without a purification step. Further details are given in the Experimental Procedures section.

SWNTs were suspended in water using sodium dodecyl sulfate (SDS), and their sidewalls were covalently functionalized. Nitrobenzene diazonium salts, after being dissolved in a small amount of CH_3CN (mono- and dinitrobenzene) or as-prepared in the acidic medium (tri-), were slowly introduced to the SWNT solution where the electron transfer from SWNTs to the diazonium species induces nitrogen evolution, followed by stable C−C bonding to the SWNT surface.[17] This covalent functionalization proceeded very fast because of the further electrodeficient character of nitrobenzene.[15] The more nitro groups the diazonium salt has, the more readily it receives electrons, thus making nitrogen loss easier. However, it also means that the stability of diazonium salts in the reaction mixture decreases proportionally to the number of nitro groups (mono < di < tri) because the more undesired reaction pathways become feasible. Thus, more concentrated reagent was needed for 2,4-dinitrophenyl functionalized SWNTs (DNP-SWNTs) than for 4-nitrophenyl SWNTs (MNP-SWNTs), if a similar level of functionalization was desired. However, for the synthesis of 2,4,6-trinitrophenyl SWNTs (TNP-SWNTs), only a certain level of functionalization was achieved before TNP-SWNTs flocculated out of the reaction mixture, mainly because of the significant instability of SDS micelles in the presence of the acid (from the diazonium salt preparation) and many decomposed byproducts. In this case, TNP-SWNTs were filtered and redispersed in a fresh SDS aqueous solution, and then the diazonium reaction was repeated to increase the level of functionalization as desired. Further details are given in the Experimental Procedures section.

Raman and FT-IR spectroscopies verified covalent functionalization of SWNTs with nitrophenyl groups (Figure 2). As expected, the covalent attachment of nitrophenyl groups increased the disorder mode (D-peak, ∼1300 cm^{-1}) in Raman spectra when compared to the graphitic mode (G-peak, ∼1590 cm^{-1}) in all cases (Figure 2a). Samples with various D/G ratios can be produced by starting with different concentrations of diazonium salts. FT-IR spectroscopy verified the existence of nitrophenyl groups on all three kinds of nitrophenyl-SWNTs (Figure 2b). Asymmetric and symmetric NO_2 stretching modes are obvious in the FT-IR spectra from the SWNT films (measured with an ATR (attenuated total reflectance) accessory).

Differential Scanning Calorimetry and Isoconversional Analysis. The energy-releasing properties of these nitrophenyl-functionalized SWNTs were demonstrated in differential scanning calorimetry (DSC) (Figure 3a).[20−22] Samples with masses from 0.5 to 0.6 mg were loaded on an aluminum pan, and the temperature was scanned from 150 to 385 at 10 °C/min under nitrogen. For comparison, SWNTs functionalized with a nonenergetic 4-bromophenyl group (BrP-SWNTs) were examined under the same conditions. The downward direction indicates an exothermic heat flow in the DSC traces presented.

When the nonenergetic BrP-SWNTs were scanned, no appreciable variation from the baseline was observed. After the sample

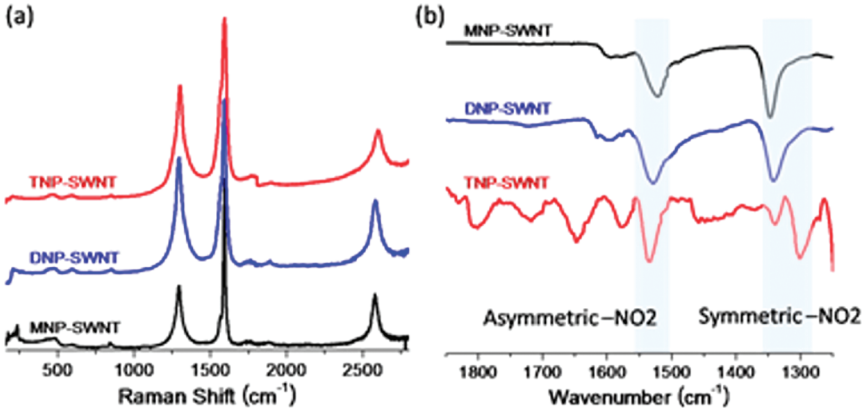

Figure 2. Raman and FT-IR characterization of energetically decorated SWNTs. (a) Disorder modes (~1200 cm^{-1}) increased in the Raman spectra after covalent functionalization (excited at 785 nm). (b) FT-IR spectra were measured on films with ATR, showing nitro groups are present. MNP-, DNP-, and TNP-SWNTs represent mono-, di-, and trinitrophenyl-functionalized SWNTs, respectively.

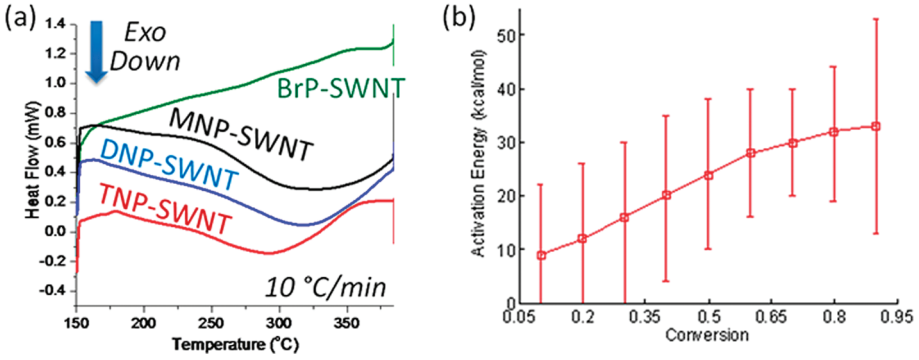

Figure 3. (a) DSC heat flow (exo down) scanned at 10 °C/min under nitrogen for BrP-SWNTs (black), MNP-SWNTs (green), DNP-SWNTs (blue), and TNP-SWNTs (red). All the nitrophenyl-SWNTs react and release heat whereas the BrP-SWNTs do not. (b) Apparent activation energy of the exothermic reaction of DNP groups covalently bonded to SWNTs increases with total conversion. DNP groups may be unevenly distributed along the SWNTs, resulting in easy energy transfer and faster reaction in concentrated clusters of DNP groups.

was subjected to a high temperature (385 °C), some 4-bromophenyl groups detached, resulting in SWNTs in nearly pristine condition. Despite thermal decomposition, no additional heat flow was found in the case of nonenergetic BrP-SWNTs. Remarkably, however, energetically decorated SWNTs appear to generate considerable heat when decomposed at high temperatures. As shown in Figure 3a, all DSC traces of MNP-, DNP-, and TNP-SWNTs showed peaks in exothermic heat flow between 300 and 330 °C as the temperature was increased. This feature highlights that energetically decorated SWNTs can be utilized as thermally induced heat-releasing elements.

It is worthy of note that the exothermic DSC peak shifts to lower temperatures as the number of nitro groups increases. This shift can be attributed to the decreasing activation energy for thermal decomposition from mono- to di-, and to trinitrophenyl moieties.[21] However, the onset of thermal decomposition occurred at a similar temperature (~170 °C) regardless of the number of attached nitrophenyl groups. The onset temperatures for NP-SWNT thermal decomposition are somewhat lower than that of the small molecule nitroaromatics; for example, when 2,4,6-trinitroaniline (also known as picramide) was subjected to the same DSC conditions, thermal decomposition started at 258 °C and the reaction finished in a very small temperature range (within 20 °C) (Supporting Information, Figure S1).

SWNTs appear to affect the exothermic thermal decomposition of attached nitrophenyl groups. Because of the complexity of condensed-phase thermal decomposition in nature, unlike reactions in the gas phase at low pressure, it is hard to figure out exactly what processes may occur here, but we suspect SWNTs serve as catalysts and/or heat conduits, decreasing the effective activation energy. Thermal decomposition of energetic materials is often a catalytic process, although it depends significantly on the thermal stimulus conditions (temperature and pressure).[21] Thus, it is reasonable to assume that defect sites on SWNTs can serve as catalytic sites. Alternatively, the high thermal conductivity of SWNTs can contribute to the thermal decomposition of energetic molecules. Applied heat or heat from exothermic reaction in a certain zone propagates rapidly to other reaction zones, lowering the apparent activation energy there.[11,23] In addition, energetic molecules covalently attached to the SWNTs undergo exothermic reactions at a wide range of temperatures (from 170 °C to >400 °C). We suspect that some reaction zones (e.g., those with defects) have a smaller (apparent) activation energy than others, which is more clearly shown in the isoconversional analysis (see below).

The energy released by reaction depends on the total number of nitro groups, which in turn depends upon the type of moiety and the level of functionalization. Integrating the area between each DSC peak and its baseline (Figure 3a) gives energy densities

dx.doi.org/10.1021/cm201947y |*Chem. Mater.* 2011, 23, 4557–4562

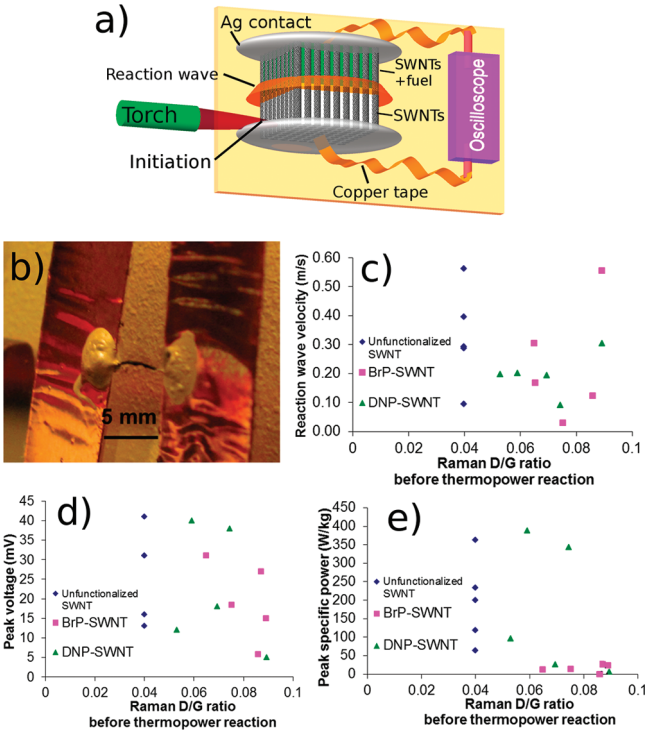

Figure 4. Thermopower waves on covalently functionalized SWNTs. (a) Schematic of a thermopower wave generator (alignment is generally less than illustrated). The thermopower reaction wave is initiated by a fine-tip torch at one end of the generator and propagates to the other contact. (b) A typical thermopower wave generator using bulk-scale SWNT fibers that have been functionalized. (c) Average velocity of thermopower waves for three different SWNT types. All supported waves with velocities between 0.03 and 0.56 m/s, regardless of level of functionalization as measured by Raman spectroscopy. (d) Peak voltage and (e) specific power of thermopower waves. Again, functionalization did not significantly affect the generation of electricity.

of 780, 600, and 440 J/g for MNP-, DNP-, and TNP-SWNTs, respectively (including the SWNT mass). It should be noted that MNP-SWNTs can often achieve greater functionalization compared to either DNP-SWNTs or TNP-SWNTs. Thus heat release can be controlled through the level of functionalization and types of energetic molecules on SWNTs, although it seems that the level of functionalization plays a bigger role here.

Isoconversional analysis[20] supports the idea that some reaction zones have a smaller apparent activation energy than others. Figure 3b shows the apparent activation energy of DNP-SWNT as a function of conversion. Three DSC experiments each were carried out at three different scanning rates (2.5, 5, 10 °C/min), for a total of nine traces that are combined in Figure 3b. Despite the large uncertainty, it is statistically valid that the activation energy at high conversion is greater than at low conversion. The uncertainty likely stems from variability in the effectiveness of the functionalization reaction, which would lead to a distribution of DNP loadings among the nine samples tested. We hypothesize that low-conversion reactions proceed via chain reactions between more reactive "islands" of higher DNP concentration along the nanotube surface. To reach higher conversions, the reaction would then have to progress to isolated DNP groups once all the islands have been depleted. The energy cost of reaching those isolated groups could plausibly explain the increase in activation energy at higher conversion.

NP-SWNTs could not support self-sustaining reaction waves without additional fuel coating, despite their energetic properties. After initiation of films of these molecules with a laser (785 nm, 40 mW) and with microwave irradiation, Raman spectroscopy observed defunctionalization of nitrophenyl groups from SWNTs in the vicinity of the irradiation spot (Supporting Information, Figure S2). However, those reactions did not propagate farther, mainly because of the heat loss to the environment; suspending NP-SWNT films resulted in longer-traveling reactions (albeit still incomplete) than those on a substrate (which acts as a heat sink) (Supporting Information, Figure S3). To overcome the heat loss, either complete thermal isolation or much higher grafting density of energetic molecules is necessary. Further details of these experiments are given in Supporting Information.

Thermopower Wave Experiments. However, DNP-SWNTs could support self-propagating reaction waves when coated with picramide (PA) and sodium azide as fuel and initiator (to decrease activation energy), respectively. Figure 4a shows a schematic of a thermopower wave generator (TWG), as described conceptually in the Introduction. Applied at both ends of a SWNT fiber, silver paste flows around and among SWNTs before drying, forming strong, highly conductive electrical connections to copper tape electrodes. A digital oscilloscope (Yokogawa DL 1735E) measures voltage generated during the reaction. Current and power then can be calculated based on the known resistances of the TWGs and the oscilloscope circuit. The progress of the reaction wave is monitored visually at 4000 frames/second using a high speed camera from Canadian Photonic Laboratories Inc. (Mega Speed, CPL-MS70KS2B90) with a Nikon, AF Micro-NIKKOR 60 mm f/2.8D macro lens. For these experiments, thermopower waves were initiated with a fine-tip butane torch.

Unfunctionalized and functionalized SWNT fibers were fueled with PA and incorporated in TWGs, as depicted in the image of Figure 4b. The fibers, obtained from KH Chemicals, contain individual SWNTs with diameters of 1.0−1.3 nm and lengths of 5−50 μm. Each fiber contains millions of SWNTs and thus is several millimeters long but does not have a well aligned internal structure. Further details of the preparation of these materials are available in the Experimental Procedures section.

The presence of functional groups and the level of functionalization did not affect the average velocity of these reaction waves. Figure 4c compares average velocities of reaction waves in picramide guided by DNP-, BrP-, and unfunctionalized SWNTs. Average velocity during reaction ranged from 0.03 to 0.56 m/s for all three types of SWNTs. This is less than the velocities measured for cyclotrimethylene-trinitramine (TNA) on multiwalled carbon nanotubes (MWNTs), which ranged from 0.15 to 2.0 m/s.[10] TNA has very similar energetic properties to picramide,[24−29] but the SWNTs are shorter and not as well aligned as the MWNTs. Hence, the difference can be attributed to decreased thermal diffusivity of the SWNT mass since it has orders of magnitude more junctions between nanotubes, which slow thermal transport. The properties and performance of MWNTs and SWNTs (functionalized and unfunctionalized) are compared in Table 1.

Likewise, functionalization did not significantly affect electrical generation from thermopower waves. Figures 4d and 4e show the peak voltage and peak specific power, respectively, from thermopower wave generators using the three different SWNT materials. In each series, peak voltage ranged from about 5 to 40 mV,

Table 1. Energetic Properties of Thermopower Wave Materials[a]

fuel/conduit	voltage, V (max)	specific power, W/kg (max)	activation energy, kJ/mol	wave velocity, m/s (max)	energy density, J/g (max)
TNA/MWNT[10]	210	7000	127[29]	2.0	3870[27]
PA/SWNT	41	360	134[26]	0.56	2380
PA/BrP-SWNT	31	30	134[26]	0.56	2840
PA/DNP-SWNT	40	390	134[26]	0.30	2650
DNP-SWNT			96 ± 56		600

[a] Energy density calculated based on reaction enthalpy of fuel, including mass of fuel, initiator (NaN_3), and conduit. The mass ratio of TNA to MWNT is 9:1. The calculations for DNP-SWNT are based on Figure 3.

and peak specific power ranged from 5 to 400 W/kg. The BrP-SWNTs all produced <30 W/kg peak specific power but not because of the functional groups. Rather, the fabrication of those generators resulted in large contact and internal resistance. The fact that BrP-SWNTs generated peak voltages in the same range as the other SWNT materials supports tracing the problem to resistance.

On the basis of the ratio of the intensity of D and G peaks, Raman spectroscopy shows that the level of functionalization is lower for the DNP- or BrP-SWNT fibers (Figure 4) than for functionalized dispersed SWNTs (Figure 2a). Nevertheless, both DNP- and BrP-SWNT fibers have larger D/G ratios than unfunctionalized fibers, confirming that covalent functionalization occurs. The covalent bonds between DNP or BrP moieties and nanotube sidewalls create electronic defects in the nanotube lattice, which should scatter phonons and electrons, decreasing SWNT conductivity. But these defects do not significantly disrupt the thermal or electrical conduction of thermopower waves, since neither reaction velocity nor specific power decreases measurably with functionalization, at least within the range of this study. This may allow SWNTs to be assembled into more complex nanostructures using covalent linker molecules[30] without disrupting their ability to conduct thermopower waves. However, Raman spectroscopy showed that, after thermopower waves on the SWNTs, D/G ratios decreased to less than their level immediately after covalent functionalization (but before thermopower wave reaction). This analysis indicates that thermopower waves break the bonds attaching the functional groups to the SWNTs without significantly damaging the SWNTs, just as with the functionalized SWNTs in the microwave irradiation experiments (Supporting Information, Figure S3).

The energy content of the functional groups also did not affect the propagation of thermopower waves. DNP has a higher enthalpy of decomposition than BrP (Figure 3), so it might be expected to lend extra energy to a thermopower wave, increasing its velocity and/or power. However, no such enhancement was measured for this loading of energetic functional groups.

CONCLUSION

In summary, we have shown that single-walled carbon nanotubes can be decorated with energetic molecules—a series of nitroaromatics—via diazonium chemistry, and investigated their energy-releasing properties by DSC. The covalent functionalization was confirmed by Raman spectroscopy, and the presence of nitro groups was observed in the FT-IR spectroscopy. Energetically decorated SWNTs release heat when thermally excited, whereas nonenergetic BrP-SWNTs demonstrated no energy output. Mono-, di-, and trinitrobenzene-functionalized SWNTs had energy densities of 780, 600, and 440 J/g, respectively, indicating that the increase in energy density per moiety with increasing number of nitro groups is not as influential as the efficiency of the functionalization reaction to overall energy density. Isoconversional analysis showed the apparent activation energy is smaller at low conversion, which may be due to a chain reaction using the SWNT as a thermal conduit. Thermopower waves propagated on decorated SWNTs with the same velocity and power as on unfunctionalized nanotubes, showing that electronic defects do not necessarily disrupt wave propagation. These highly promising nanoenergetic materials demonstrate 1-D reaction propagation and directional energy release, and they can serve as on-demand nanoscale energy sources that can be remotely activated.

EXPERIMENTAL PROCEDURES

Materials. As-produced SWNTs were purchased from Unidym (Menlo Park, CA), synthesized by a high-pressure CO decomposition process (HiPCO), or from Nano-C (Westwood, MA), synthesized by its combustion-based technology. SWNTs were suspended in 1% sodium dodecyl sulfate (SDS) in Milli-Q water (initially ~0.4 mg/mL), homogenized for 1 h (6500 rpm), cup-horn sonicated for 10 min at 90% power, and ultracentrifuged at 30000 rpm for 4 h to isolate individual SWNTs from bundles. Anhydrous acetonitrile (CH_3CN) was purchased from Aldrich in Sure-Seal Bottles and used as received. 4-Nitrobenzenediazonium tetrafluoroborate (MNP-$N_2^+BF_4^-$) was purchased from Sigma-Aldrich (St Louis, MO). 2,4-Dinitrobenzenediazonium tetrafluoroborate (DNP-$N_2^+BF_4^-$)[15,31] and 2,4,6-trinitroaniline[32] were synthesized by a known procedure. All other chemicals were reagent grade and used as received.

Synthesis of 2,4,6-Trinitrobenzenediazonium Hydrogen Sulfate (TNP-$N_2^+HSO_4^-$). Sodium nitrite (1.65 g, 24 mmol) was dissolved in sulfuric acid (10 mL) to produce nitrosylsulfuric acid. To a solution of 2,4,6-trinitroaniline (4.56 g, 20 mmol) in AcOH (10 mL) the nitrosylsulfuric acid was added dropwise at room temperature, and the mixture was stirred for 3 h to complete the diazotization. The mixture was used in the next step without further purification. The existence of the diazonium group was verified by an azo dye test with 2-naphthol.[33]

Synthesis of Nitrophenyl-functionalized SWNTs (NP-SWNTs). To a stirred solution of SDS-suspended SWNTs (40 mL) was added nitrobenzenediazonium tetrafluoroborate (5 mM, 47 mg for mono- or 56 mg for dinitro-) in portions over 2 h at 50 °C. In case of 2,4,6-trinitrophenyl-SWNTs, an acidic solution of TNP-$N_2^+HSO_4^-$ (5 mM, 0.2 mL) was added dropwise over 2 h. The reaction was monitored by Raman spectroscopy. After 4 h, the mixture was cooled to room temperature, diluted with acetone (40 mL) to facilitate filtration through a PTFE membrane filter. After washing with water (40 mL, twice) and acetone (40 mL), the product NP-SWNTs were redispersed in dimethylformamide (20 mL) by gentle sonication for 10 min. The product was filtered again through PTFE and again washed with water (40 mL, twice) and acetone (40 mL) to remove residual surfactant and byproducts. The purified NP-SWNTs were then dried in air.

dx.doi.org/10.1021/cm201947y |Chem. Mater. 2011, 23, 4557–4562

Dinitrophenyl-Functionalization of Single-Walled Carbon Nanotube Fibers (DNP-SWNTs). SWNT fibers (~0.5 mg) were placed in 1% sodium dodecyl sulfate in water (~1 mL). To the solution was added dinitrobenzenediazonium tetrafluoroborate (DNP-$N_2^+BF_4^-$, 1.35 mg, 5 mM). The mixture was gently stirred at 45 °C for 6 h, at which time the functionalized SWNT fibers were washed three times each in acetone and water successively to remove any adsorbed reagents and SDS. The functionalized SWNT fibers were dried in air and characterized. BrP-SWNTs were produced in the same fashion using BrP-$N_2^+BF_4^-$.

Instrumentation. Raman spectra were measured by Horiba Jobin Yvon LabRAM HR800 with a microscope and 633- or 785-nm laser excitation. Because of heterogeneities in the SWNT fibers, each thermopower wave generator was measured in three different locations, and the resulting D/G ratios were averaged. FT-IR spectra were obtained using a Thermo Nicolet 4700 spectrometer with an ATR accessory. Heat flows in differential scanning calorimetry (DSC) were determined using a TA Instrument Q100 under nitrogen atmosphere.

Thermopower Wave Generator Preparation. PA (15 g/L in acetonitrile) and sodium azide (10 or 20 g/L in water) solutions were dropped on the fibers in turn, allowing several hours for solvent evaporation after addition of each solution. Each thermopower wave generator (TWG) was loaded with about three times as much PA as SWNTs by mass and one to two times as much NaN_3 as SWNTs. TWG resistances ranged from 1.5 to 162 Ω depending on length and width of the SWNT fibers.

■ ASSOCIATED CONTENT

Supporting Information. DSC trace of 2,4,6-trinitroaniline, Raman spectra, and high-speed images of nitrophenyl-SWNTs initiated by microwave and laser excitation. This material is available free of charge via the Internet at http://pubs.acs.org.

■ AUTHOR INFORMATION

Corresponding Author
*E-mail: strano@mit.edu.

Author Contributions
⊥These authors contributed equally to this work.

■ ACKNOWLEDGMENT

This work was supported by Air Force Office of Scientific Research Grant FA9550-09-1-0700 and a National Science Foundation Graduate Research Fellowship for J.T.A. C.S. thanks Sungkyunkwan University. W.C. thanks the ILJU Foundation of Education and Culture for fellowship support.

■ REFERENCES

(1) Arico, A. S.; Bruce, P.; Scrosati, B.; Tarascon, J.-M.; van Schalkwijk, W. *Nat. Mater.* **2005**, *4*, 366.
(2) Liu, J.; Cao, G.; Yang, Z.; Wang, D.; Dubois, D.; Zhou, X.; Graff, G. L.; Pederson, L. R.; Zhang, J.-G. *ChemSusChem* **2008**, *1*, 676.
(3) Baxter, J.; Bian, Z.; Chen, G.; Danielson, D.; Dresselhaus, M. S.; Fedorov, A. G.; Fisher, T. S.; Jones, C. W.; Maginn, E.; Kortshagen, U.; Manthiram, A.; Nozik, A.; Rolison, D. R.; Sands, T.; Shi, L.; Sholl, D.; Wu, Y. *Energy Environ. Sci.* **2009**, *2*, 559.
(4) Rolison, D. R.; Long, J. W.; Lytle, J. C.; Fischer, A. E.; Rhodes, C. P.; McEvoy, T. M.; Bourg, M. E.; Lubers, A. M. *Chem. Soc. Rev.* **2009**, *38*, 226.
(5) *Nanoparticle Assemblies and Superstructures*; Kotov, N. A., Ed.; CRC Press: Boca Raton, FL, 2006.
(6) *The Chemistry of Nanomaterials: Synthesis, Properties and Applications*; Rao, C. N. R., Muller, A., Cheetham, A. K., Eds.; Wiley-VCH: Weinheim, Germany, 2004.
(7) Dlott, D. D. *Mater. Sci. Technol.* **2006**, *22*, 463.
(8) Armstrong, R. W.; Baschung, B.; Booth, D. W.; Samirant, M. *Nano Lett.* **2003**, *3*, 253.
(9) Abrahamson, J. T.; Nitish, N.; Strano, M. S. *Nanotechnology* **2008**, *19*, 195701.
(10) Choi, W.; Hong, S.; Abrahamson, J. T.; Han, J.-H.; Song, C.; Nair, N.; Baik, S.; Strano, M. S. *Nat. Mater.* **2010**, *9*, 423.
(11) Choi, W.; Abrahamson, J. T.; Strano, J. M.; Strano, M. S. *Mater. Today* **2010**, *13*, 22.
(12) Abrahamson, J. T.; Choi, W.; Schonenbach, N. S.; Park, J.; Han, J.-H.; Walsh, M. P.; Kalantar-zadeh, K.; Strano, M. S. *ACS Nano* **2011**, *5* (1), 367–375.
(13) Walia, S.; Weber, R.; Latham, K.; Petersen, P.; Abrahamson, J. T.; Strano, M. S.; Kalantar-zadeh, K. *Adv. Funct. Mater.* **2011**, *21*, 2072.
(14) Strano, M. S.; Dyke, C. A.; Usrey, M. L.; Barone, P. W.; Allen, M. J.; Shan, H. W.; Kittrell, C.; Hauge, R. H.; Tour, J. M.; Smalley, R. E. *Science* **2003**, *301*, 1519.
(15) Nair, N.; Kim, W.-J.; Usrey, M. L.; Strano, M. S. *J. Am. Chem. Soc.* **2007**, *129*, 3946.
(16) Graff, R. A.; Swanson, T. M.; Strano, M. S. *Chem. Mater.* **2008**, *20*, 1824.
(17) Usrey, M. L.; Lippmann, E. S.; Strano, M. S. *J. Am. Chem. Soc.* **2005**, *127*, 16129.
(18) Smith, L. I.; Paden, J. H. *J. Am. Chem. Soc.* **1934**, *56*, 2169.
(19) Takagishi, I.; Hashida, Y.; Matsui, K. *Bull. Chem. Soc. Jpn.* **1979**, *52*, 2635.
(20) Long, G. T.; Brems, B. A.; Wight, C. A. *Thermochim. Acta* **2002**, *388*, 175.
(21) Brill, T. B.; James, K. J. *Chem. Rev.* **1993**, *93*, 2667.
(22) Cohen, R.; Zeiri, Y.; Wurzberg, E.; Kosloff, R. *J. Phys. Chem. A* **2007**, *111*, 11074.
(23) Nair, N.; Strano, M. S. *Phys. Rev. B* **2009**, *80*, 174301.
(24) Brill, T. B.; James, K. J. *J. Phys. Chem.* **1993**, *97*, 8752.
(25) Liau, Y. C.; Kim, E. S.; Yang, V. *Combust. Flame* **2001**, *126*, 1680.
(26) Maksimov, Y. Y.; Kogut, E. N. *Russ. J. Phys. Chem.* **1978**, *52*, 805.
(27) Volkov, E. N.; Paletsky, A. A.; Korobeinichev, O. P. *Combust. Explos. Shock Waves* **2008**, *44*, 43.
(28) Parr, T.; Hanson-Parr, D. *Twenty-Seventh Symposium (International) on Combustion*; Combustion Inst., 1998; Vols. 1 and 2, p 2301.
(29) Williams, M. R.; Matei, M. V. *Propellants, Explos., Pyrotech.* **2006**, *31*, 435.
(30) Song, C.; Kwon, T.; Han, J.-H.; Shandell, M.; Strano, M. S. *Nano Lett.* **2009**, *9*, 4279.
(31) Broxton, T. J.; Colton, R.; Traeger, J. C. *J. Phys. Org. Chem.* **1995**, *8*, 351.
(32) Rosevear, J.; Wilshire, J. *Aust. J. Chem.* **1985**, *38*, 723.
(33) Conant, J. B.; Lutz, R. E.; Corson, B. B. *Org. Synth., Collective Volume 1* **1941**, 49.